Cardiovasc Eng (2010) 10:84–90
DOI 10.1007/s10558-010-9096-x

TECHNICAL NOTE

New Insights into Pacemaker Lead-Induced Venous Occlusion: Simulation-Based Investigation of Alterations in Venous Biomechanics

Anna Lonyai · Anne M. Dubin · Jeffrey A. Feinstein · Charles A. Taylor · Shawn C. Shadden

Published online: 1 June 2010

Abstract Venous obstruction is a major complication of transvenous pacemaker placement. Despite the increasing use of pacemakers and implantable cardiac defibrillators, a lack of understanding remains with regard to risk factors for the development of device-associated venous obstruction. We hypothesize that computational fluid dynamics simulations can reveal prothrombogenic locations and define thrombosis risk based on patient-specific anatomies. Using anatomic data derived from computed tomography, computer models of the superior vena cava, subclavian, innominate, and internal jugular veins were constructed for three adult patients with transvenous pacemakers. These models were used to perform patient-specific simulations examining blood flow velocity, wall shear stress, and blood pressure, both with and without the presence of the pacing leads. To better quantify stasis, mean exposure time fields were computed from the venous blood flow data. In comparing simulations with leads to those without, evident increases in stasis at locations between the leads and along the surface of the vessels closest to the leads were found. These locations correspond to regions at known risk for thrombosis. This work presents a novel application of computational methods to study blood flow changes induced by pacemaker leads and possible complications such as venous occlusion and thrombosis. This methodology may add to our understanding of the development of lead-induced thrombosis and occlusion in the clinical arena, and enable the development of new strategies to avoid such complications.

Keywords Venous occlusion · Pacemaker leads · Computational fluid dynamics

A. Lonyai
School of Medicine, Stanford University, Palo Alto, CA, USA

A. M. Dubin · J. A. Feinstein
Department of Pediatrics–Division of Cardiology, Stanford University, Palo Alto, CA, USA

J. A. Feinstein · C. A. Taylor
Department of Bioengineering, Stanford University, Palo Alto, CA, USA

S. C. Shadden (✉)
Mechanical, Materials and Aerospace Engineering, Illinois Institute of Technology, 10 W. 32nd St, Chicago, IL 60616, USA
e-mail: shawn.shadden@iit.edu

Introduction

In 2006, there were 418,000 pacemakers and 114,000 implantable cardiac defibrillators (ICDs) implanted in the United States and these numbers continue to rise (Lloyd-Jones et al. 2009). Despite their increasing use, a lack of understanding remains with regard to risk factors for the development of device-associated venous obstruction. Significant obstruction following transvenous pacemaker implantation is common, being reported in 14 to 37% of cases (Haghjoo et al. 2007; Korkeila et al. 2007; Oginosawa et al. 2002; Sticherling et al. 2001). These obstructions may lead to superior vena cava syndrome (Goudevenos et al. 1989; Mazzetti et al. 1993) or, with a 0.4–0.8% chance of fatal or near fatal complications, make pacemaker lead replacement or removal difficult and dangerous (Byrd et al. 2002; Smith et al. 1994; Wilkoff et al. 2005, 1999). These issues are especially concerning for children, due to their smaller vessels and the need for life-long pacing.

Limited and conflicting data on the risk factors associated with venous occlusion following pacemaker lead implantation exist. Bar-Cohen concluded that occlusion

was independent of the number or size of leads, or the duration of time the leads had been in place (Bar-Cohen et al. 2006). Others, however, suggest that the number of leads is a significant predictor of venous thrombosis and occlusion (Figa et al. 1997; van Rooden et al. 2004). In addition, these and other studies investigating venous thrombosis after pacemaker implantation show large variations in rates of venous thrombosis and call attention to the limited information we have on identifying key risk factors (Rozmus et al. 2005).

A novel method to study flow conditions in the cardiovascular system is the application of patient-specific computational blood flow simulation. Simulation-based modeling has been used with success to predict blood flow characteristics following surgical procedures, including bypasses for peripheral arterial disease (Taylor et al. 1999) and aortoiliac occlusive disease (Wilson et al. 2005), and, in the arena of congenital heart disease, for the Fontan procedure among others (Marsden et al. 2009). To our knowledge this framework has not been utilized to characterize blood flow conditions in the venous system of patients after transvenous pacemaker implantation. This perspective enables a remarkable level of detail on flow conditions not possible from current image-based methods, the ability to consider patient-specific anatomic differences, and the ability to explore potential benefits of altering design parameters. In this paper we examine how lead implantation influences local blood flow conditions as it relates to inducing stasis and, potentially, occlusion.

Specifically, we investigate in patient-specific anatomies the effect of lead placement in the venous system by comparing computational models of blood flow in the presence and absence of transvenous leads. While there are many factors that may affect risk for thrombosis, in this work we focus on hemodynamic factors, specifically changes in velocity, pressure, and shear stress in the veins, and locate and quantify regions of stasis to identify where potential risk for thrombosis occurs. We believe the identification of these regions is critical to predicting and preventing areas of thrombosis and occlusion in a patient-specific manner.

Methods

Computed Tomography

Computed tomography (CT) was used to obtain high-resolution anatomic information from three patients with pacemakers. A thin-section, first-pass, contrast-enhanced CT angiographic technique was employed to produce high-resolution, three-dimensional image data of the vascular anatomy surrounding the leads. Patient 1 was scanned with a 64-slice multidetector CT scanner (Somatom Sensation 64, Siemens, Forchheim, Germany), which produced 1 mm thick images. Patients 2 and 3 were scanned with a 16-slice multidetector CT scanner (LightSpeed 16, GE, Milwaukee, Wisconsin), which produced 1.25 mm thick images. In all cases, 2 cc kg^{-1} of Omnipaque was administered intravenously at a rate $\geq$3 cc s^{-1}. When the central venous system was opacified by the contrast agent, a breath-held spiral scan of the chest was obtained from the thoracic inlet to the base of the diaphragm. Continuous images were then reconstructed for post-processing.

Computational Fluid Dynamics

The techniques for construction of vascular models from medical image data has been described previously.(Wilson et al. 2001, 2005) In summary, models of the superior vena cava (SVC), left and right subclavian (L/R-SC), left and right innominate (L/R-Inn), and left and right internal jugular (L/R-IJ) veins were constructed by the following steps (see Fig. 1): (1) paths were defined along the center of each vessel of interest, (2) the vessel lumen was determined at discrete locations along each path, (3) these lumen segments were lofted to create a 3D geometric model of the vascular anatomy, and (4) this geometric model was discretized into a finite element mesh for use with custom computational fluid dynamics (CFD) software. For each patient, two models were constructed: one from the vasculature data alone and another that contained the pacing leads. The centerline paths of the leads were determined from the CT data and the leads were reconstructed by assuming a constant cross-sectional area. The finite-element mesh used to solve the governing equations for blood flow was constructed from tetrahedral elements with a 0.05 cm nominal edge size. This resulted in total mesh sizes of approximately 2–3 million elements without leads, and slightly larger mesh sizes for the models containing the leads.

Blood flow was simulated by solving the Navier–Stokes equations (NSE) over the model using a stabilized finite-element method (Taylor et al. 1998a, b). Based on available literature, an SVC flow rate of 1.8 L min^{-1}, adjusted for body surface area, was prescribed with equal distribution among the subclavian and internal jugular veins (Mohiaddin et al. 1990). A resistance boundary condition was imposed at the SVC outlet to represent the downstream vasculature. The resistance was set to 290 dynes s cm^{-5} to achieve a physiologic pressure of 5 mmHg at the entrance of the right atrium. A no-slip boundary condition was imposed along the walls of the vessels and the leads. The computed solutions yield highly-resolved pressure and velocity fields in the interior of the lumen and shear stress along the walls.

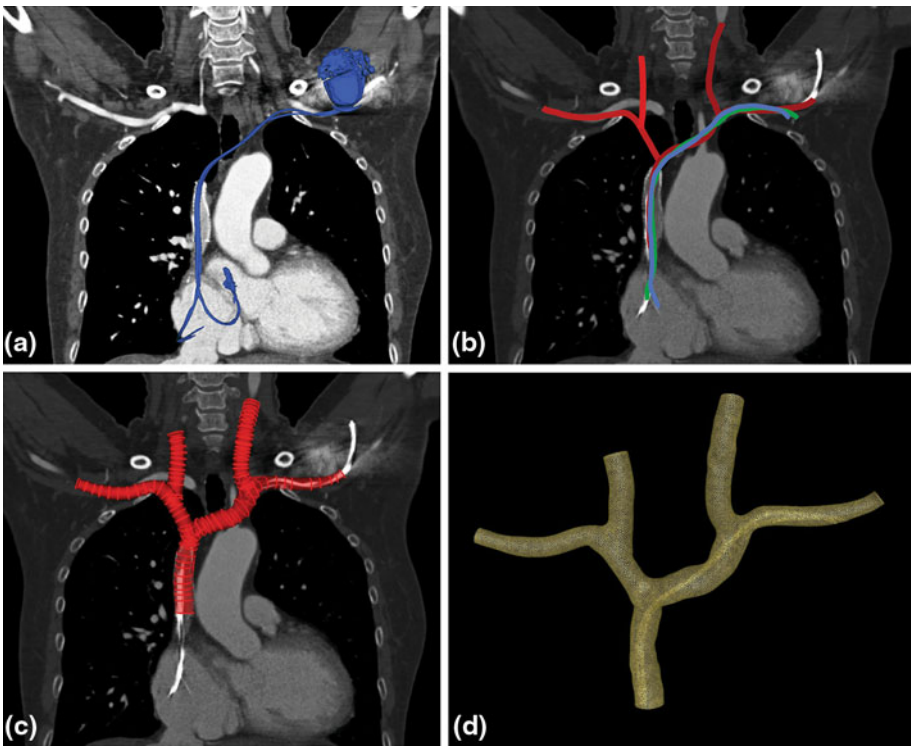

Fig. 1 Process overview. **a** Patient-specific CT image with pacemaker leads and generator highlighted. **b** Paths drawn through the center of the great veins (*red*) and leads (*green and blue*) (Note: paths are not entirely in CT section plane and have been drawn overly thick for demonstration purposes). **c** The vessel lumen is defined (i.e. traced) at fixed intervals along each vessel (segmented) and these slices are lofted together to provide a geometric model of the great veins and pacemaker leads. **d** High-resolution computational mesh is created from the geometric model

Mean Exposure Time Computations

The mean exposure time (MET) field was computed in each model by releasing a high concentration of fluid particles at the inlets and measuring how long each particle resided in particular regions. More specifically, the finite element mesh used to solve the NSE discretizes the vessel into a set of sub-domains—millions of tetrahedral volumes or elements. A dense, spatially-uniform concentration of fluid particles flowed in from the inlets of the model. The path of each particle was tracked as it flowed through the vasculature. For each element of the model (i.e. sub-domains) the average amount of time all of the particles spend in that element is tracked. This value is then normalized by the volume of the element as the amount of time spent in an element is proportional to, among other things, the size of the element. Mathematically, the MET for an element e is given by

$$\mathrm{MET}_e = \frac{1}{\mathrm{N}_e \mathrm{V}_e} \sum_{p=1}^{\mathrm{N}_t} \int_0^{\infty} \mathrm{H}_e^p(t)\mathrm{dt}$$

where N_e is the number of encounters of a particle passing through element e, V_e is the volume of element e, N_t is the total number of particles released, and $\mathrm{H}_e^p(\mathrm{t})$ is equal to 1 if particle p is located inside element e at time t and is equal to 0 otherwise. Note that the contribution from recirculating particles accumulates if the particles pass through the same element multiple times (Fig. 2). This property is desirable since stagnation due to recirculation is believed to be clinically significant. However, under this framework, a vigorously recirculating particle would contribute less to the MET than stagnation caused by low flow rate. For example, a particle that passes though an element twice, each pass spanning 1 time unit, does not contribute as much to the MET as a particle passing through once for two time units. While there is no universal law to support this weighting, intuition dictates that the proposed measure should capture stagnation both due to low flow and recirculation, with vigorous recirculation being a lower risk than stagnation.

Results

Patient Population

Three patients (mean age 73 years, 2 female) with dual chamber pacemakers were selected from an adult pacemaker database. Patient characteristics are shown in Table 1 and their anatomies represented a wide range of normal venous anatomy.

Velocity Field

We considered four specific cross-sections: one in the R-Inn, one in the SVC just after the junction of the innominate, one in the L-Inn at one-third the distance between the SVC and

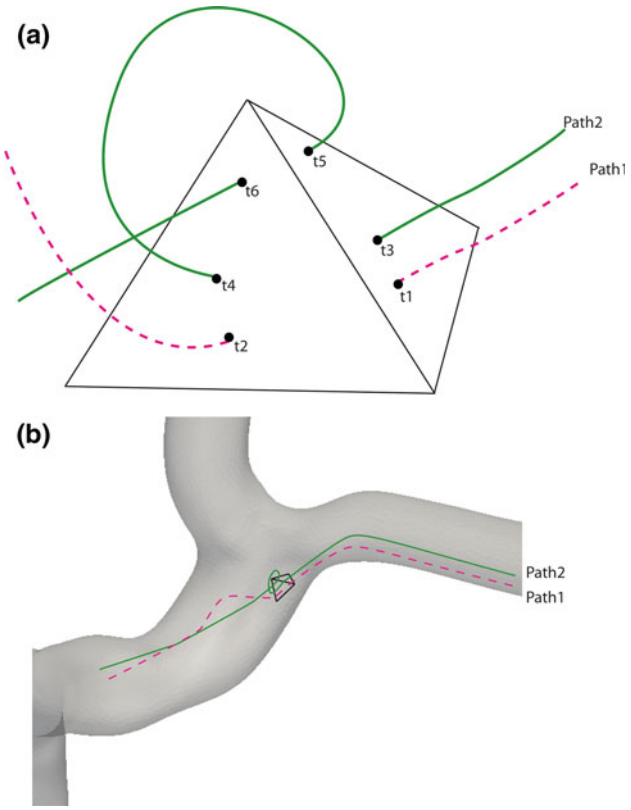

Fig. 2 Illustration of MET concept for a representative tetrahedral element. **a** Path1 (dashed) passes through the tetrahedral only once, from time t1 to t2, while Path2 (*solid, green*) passes through tetrahedral twice, from times t3–t4 then t5 to t6. Both are included in the calculations of the MET. **b** Represents the element and two paths in the context of a portion of the complete model

Table 1 Patient demographics

Patient	Age	Sex	BSA (m^2)	Pacing indications
1	58	F	1.58	Complete heart block
2	85	F	1.61	Trifascicular block
3	75	M	1.87	Atrial fibrillation

BSA Body surface area

IJ, and one at the IJ-SC junction (Fig. 3). We report these cross-sections based on our clinical experience and previous studies of sites where thrombosis tends to occur in these patients with pacemaker leads (Bar-Cohen et al. 2006). In addition, cross-sections throughout the model were examined and found to have either the same or smaller differences in velocity, shear stress and MET overall between lead and non-lead conditions.

As could be expected, in the R-Inn, there was no significant difference in the distribution of the velocity field between lead and no-lead conditions in all three models and serves, in effect, as an internal control. At the entrance to the SVC, Patient 1 showed the greatest change in velocity distribution when leads were introduced, revealing areas with as much as a doubling of the velocity (15 to 30 cm s^{-1}) as well as areas of reduced velocity between the leads and the vessel wall. In the SVC for Patient 2, the leads were placed relatively close together and near the side of the vessel wall predisposing them to a relatively high flow. The resulting flow rate near the leads remained relatively high, except in the immediate vicinity between the leads and between the leads and vessel wall. In the SVC of Patient 3, the leads were placed away from the vessel wall with relatively large spacing between the leads; this maintained moderate flow rates in the vicinity of the leads and near the vessel wall.

In some areas of the cross-sections of the L-Inn of Patient 1 and 2 there were increases in the magnitude of velocity of up to 50–100% when the leads were present at the two locations considered. Patient 3 showed a smaller increase in velocity in those cross-sections between lead and no-lead cases (about 25–50% increase). In general, leads placed at locations where flow rates were relatively low in the no-lead condition perpetuated the flow stasis. The velocity magnitude across the entire model ranged from 22.5 cm s^{-1} for Patient 3, to 32.9 cm s^{-1} for Patient 2.

Shear Stress Distribution

In all patients, the mean wall shear stress (MWSS) across the entire model (excluding the shear stress on the lead walls) was about 25% higher in the case with leads than without leads (Fig. 4). The R-Inn showed about the same WSS in the lead and no-lead condition, however, there was a marked increase in WSS in the L-Inn and SVC in all models. To better demonstrate this variation, the WSS between lead and no-lead conditions was averaged over 0.5 cm segments in the SVC, R-Inn and L-Inn. The differences in the L-Inn and SVC ranged from 0.22 to 6.25 dynes cm^{-2}, with a mean increase across both veins of 2.09 dynes cm^{-2} with the introduction of leads. The difference in MWSS in the R-Inn between lead and no-lead conditions in all three cases was less than 0.17 dynes cm^{-2}. There were noticeable pockets of low WSS in regions corresponding to areas of low velocity and residence time.

Pressure Field

The overall pressure differences between lead and no-lead conditions were minimal for all three models (results not shown). The reason for this is that the downstream resistance imposed by the outlet boundary condition is much larger than the additional resistance introduced by the leads. The greatest pressure difference was found in the left SC, where pressures increased by 0.35–0.5 mm Hg in the presence of leads.

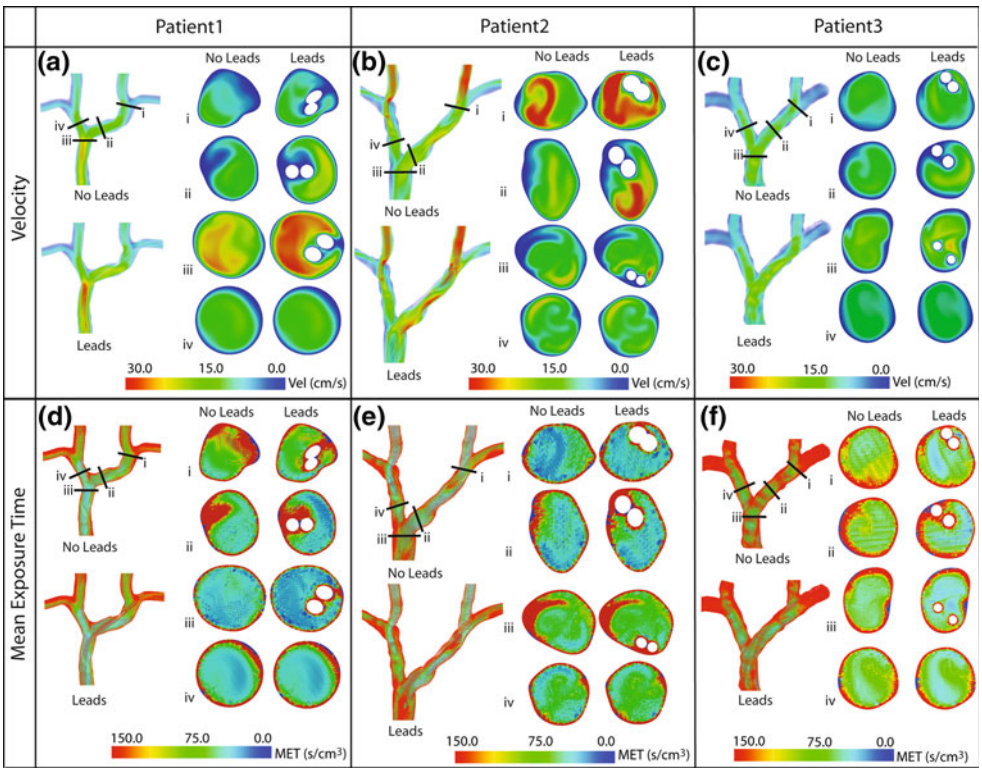

Fig. 3 Comparison of velocity and mean exposure time distributions for three patients with and without the presence of the pacing leads. **a–c** Volume rendering of the magnitude of the velocity field, including the distribution at four cross-sections (i–iv); **d–f** volume rendering of the mean exposure time field and the distribution at four cross-sections (i–iv)

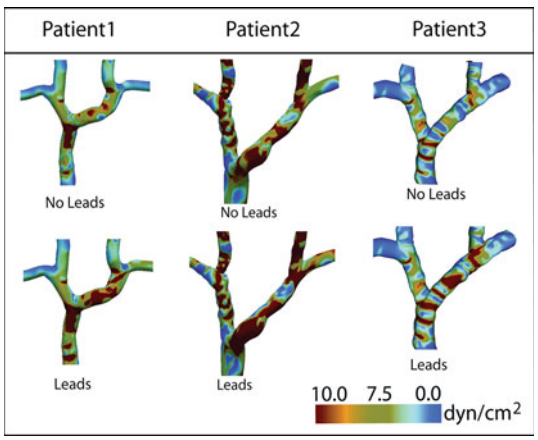

Fig. 4 Comparison of mean wall shear stress (MWSS) distributions with and without the presence of pacing leads. Volume rendering of the magnitude of the MWSS is shown for three patients with and without pacing leads

Mean Exposure Time Field

For MET computations, the spacing between particles released was 0.00125 cm, or 1/40 of the maximum edge size of the elements, generating a high-concentration of released particles. In particular, this spacing resulted in 2.1, 1.4 and 3.9 million particles being released in Patient 1, 2 and 3, respectively. In both lead and no-lead simulations, there was higher exposure (or residence) time at the junction of vessels and near the vessel walls when compared to the center of the vessel. In addition, increased MET was found immediately adjacent to the leads and in between the pacemaker lead and vessel wall, while decreased MET was noted near the center of the lumen. As shown in Fig. 3, MET distributions were examined at the four cross-sections described above in the analysis of the velocity field data. There was a dramatic increase in MET adjacent to the leads when compared to the no-lead case. Furthermore, the region between the leads and the vessel shows a large increase in MET compared to the same region without leads. This was particularly prominent in Patient 1 (Fig. 3d). The cross-section in the R-Inn vein showed no significant difference between lead and no-lead cases.

Discussion

We have demonstrated a novel application of computational blood flow simulation techniques to examine hemodynamic conditions and potential thrombosis risk in pacemaker patients. These techniques may enable improved prediction of thrombosis and subsequent vascular occlusion and, as a result, the ability to develop strategies to avoid these complications. Our method was two-pronged: (1) create a patient-specific anatomic model based on CT data and use computational fluid dynamics to investigate standard biomechanical properties such as velocity, shear stress and pressure in lead and no-lead conditions; and (2) use a newly applied method to determine the total

time particles (representing blood components such as, for example, platelets) spend in any given part of the model (i.e. vessel) under the theory that areas of high MET represent areas of high stasis and thus correlate to locations at risk for thrombosis.

Our results show that pacemaker lead placement can often result in pockets of low velocities between the leads and the vessel wall. The MET calculations confirms that in these locations blood becomes trapped for relatively long times. While overall we expected higher shear stress due to higher velocities induced by the leads, we found pockets of low shear stress in the same areas of low velocity and high MET. These low shear stress regions may also indicate areas at risk for thrombosis due to endothelial reorganization and venous stasis. Studies have indicated that low shear stress induces aggregation of leukocytes on endothelium and a consequent upregulation of inflammatory markers like tissue factor that may increase risk for thrombosis (Dormandy 1996; Nohe et al. 2005).

Interestingly, clinical data, localizing regions of occlusion, confirm areas we found to be at higher risk. Bar-Cohen clinically observed thrombosis in the SVC−Inn junction, IJ-SC junction and within the L-Inn (Bar-Cohen et al. 2006). In the present study, a combination of low velocity, high MET, and low shear stress was observed in these regions. The vicinity near vessel bifurcations may be especially at risk in venous anatomies where the lead interacts with the curvature of the vessels so as to produce a shielded region where prothrombotic cells can accumulate, such as the IJ-SC junction in Patient 1.

Overall, the positioning of leads in locations where the velocity is relatively high in the no-lead condition (presumably the preoperative state), results in relatively high flow rate and low stasis near the leads. Alternatively, lead placement near regions of low flow rate in the no-lead condition often results in obvious flow stasis near the leads. This suggests this method could be useful in trying to predict what lead positions would best minimize flow stasis. Based on our results, we would predict that positioning the leads in the highest flow regions for a given patient would minimize regions of stagnation for that individual. Peripherally, we found that lead placement does not influence the local flow conditions in upstream vessels that do not contain the leads such as the R-Inn. This suggests that if, for instance, there were an area of stenosis, leads could be placed on the opposite side with minimal upstream hemodynamic affect and, consequently, risk to that upstream stenotic vessel. Placing leads in strategic locations is, of course, not possible currently as no mechanism exists for placing leads with anything but the grossest of accuracy as it relates to their location within the lumen.

Our method enables us to establish, in a patient-specific way, the locations that may be at greatest risk for thrombosis. Previous attempts to characterize risk factors for thrombosis and occlusion have focused on global parameters such as the number of leads or size of the leads. However, thrombus tends to localize and is not uniformly distributed over the lead, which suggests that local flow plays an influential role. By using computational fluid dynamics, even in the setting of the same number and size of leads, differing risk factors can be determined for patients with different anatomies and lead positions.

While this method and these results are encouraging, we would like to point out the following limitations. Patients with pacemaker leads have varied forms of disease that affect cardiac chamber size and function. For this analysis, these changes would be modeled using alternative boundary conditions. The appropriate parameters to apply as boundary conditions have not, as yet been defined and the process to do so is poorly understood. Therefore to limit the complexity of the this study, we assume "baseline" or "representative" boundary conditions and did not explicitly model particular pacemaker-warranting disease etiologies. Further models need to be developed in patients of differing sizes and anatomy to validate the method over a wider range of individuals. Additionally, while phase contrast MRI is a common modality to determine volumetric blood flow rate, this approach was not possible for this study due to the presence of the leads. Consequently the volumetric flow rate used in this analysis was obtained from literature and adjusted for the body surface area of each patient. These inflow rates were assumed constant and assigned to the inlets of the model. Given the flow rate in the venous system is significantly less pulsatile than in arterial vessels, we consider this assumption reasonable, especially for an initial analysis. Although the inflow is steady, it should be noted that, downstream from the inlets of the model, unsteady flow occurs due to the vascular anatomy, which is accounted for in the MET computations. Nonetheless effects of respiration should be considered in future, more refined models. Also in our simulation we assumed the vessel and lead walls were rigid. Incorporating deformable wall models, as these techniques are better developed, will be desirable for future studies. Finally, we recognize, given among other limitations, clinically- relevant values for MET and shear stress are not well established, our results will require prospective, longitudinal clinical correlation.

Conclusion

Patient specific computer modeling of flow conditions resulting from pacemaker lead placement is a novel application of a well-developed method to better understand complications such as venous occlusion and thrombosis. In

addition to improving our understanding of the development of lead-induced thrombosis and occlusion in the clinical arena, this model may help in the development of new strategies to avoid these complications.

Acknowledgments The authors would like to sincerely thank Dr. Paul J. Wang for assistance with manuscript editing. This work was supported by the Stanford School of Medicine Medical Scholars Program.

References

Bar-Cohen Y, Berul CI, Alexander ME, Fortescue EB, Walsh EP, Triedman JK, Cecchin F. Age, size, and lead factors alone do not predict venous obstruction in children and young adults with transvenous lead systems. J Cardiovasc Electrophysiol. 2006;17:754–9.

Byrd CL, Wilkoff BL, Love CJ, Sellers TD, Reiser C. Clinical study of the laser sheath for lead extraction: the total experience in the United States. Pacing Clin Electrophysiol. 2002;25:804–8.

Dormandy JA. Influence of blood cells and blood flow on venous endothelium. Int Angiol. 1996;15:119–23.

Figa FH, McCrindle BW, Bigras JL, Hamilton RM, Gow RM. Risk factors for venous obstruction in children with transvenous pacing leads. Pacing Clin Electrophysiol. 1997;20:1902–9.

Goudevenos JA, Reid PG, Adams PC, Holden MP, Williams DO. Pacemaker-induced superior vena cava syndrome: report of four cases and review of the literature. Pacing Clin Electrophysiol. 1989;12:1890–5.

Haghjoo M, Nikoo MH, Fazelifar AF, Alizadeh A, Emkanjoo Z, Sadr-Ameli MA. Predictors of venous obstruction following pacemaker or implantable cardioverter-defibrillator implantation: a contrast venographic study on 100 patients admitted for generator change, lead revision, or device upgrade. Europace. 2007;9:328–32.

Korkeila P, Nyman K, Ylitalo A, Koistinen J, Karjalainen P, Lund J, Airaksinen KE. Venous obstruction after pacemaker implantation. Pacing Clin Electrophysiol. 2007;30:199–206.

Lloyd-Jones D, Adams R, Carnethon M, De Simone G, Ferguson TB, Flegal K, Ford E, Furie K, Go A, Greenlund K, Haase N, Hailpern S, Ho M, Howard V, Kissela B, Kittner S, Lackland D, Lisabeth L, Marelli A, McDermott M, Meigs J, Mozaffarian D, Nichol G, O'Donnell C, Roger V, Rosamond W, Sacco R, Sorlie P, Stafford R, Steinberger J, Thom T, Wasserthiel-Smoller S, Wong N, Wylie-Rosett J, Hong Y. Heart disease and stroke statistics–2009 update: a report from the American Heart Association Statistics Committee and Stroke Statistics Subcommittee. Circulation. 2009;119:e21–181.

Marsden AL, Bernstein AJ, Reddy VM, Shadden SC, Spilker RL, Chan FP, Taylor CA, Feinstein JA. Evaluation of a novel Y-shaped extracardiac Fontan baffle using computational fluid dynamics. J Thorac Cardiovasc Surg. 2009;137:394–403 e392.

Mazzetti H, Dussaut A, Tentori C, Dussaut E, Lazzari JO. Superior vena cava occlusion and/or syndrome related to pacemaker leads. Am Heart J. 1993;125:831–7.

Mohiaddin RH, Wann SL, Underwood R, Firmin DN, Rees S, Longmore DB. Vena caval flow: assessment with cine MR velocity mapping. Radiology. 1990;177:537–41.

Nohe B, Johannes T, Schmidt V, Schroeder TH, Kiefer RT, Unertl K, Dieterich HJ. Effects of reduced shear stress on inflammatory reactions in vitro. Effects of pathological flow conditions on leukocyte-endothelial interactions and monocyte tissue factor expression in human cell cultures. Anaesthesist. 2005;54:773–80.

Oginosawa Y, Abe H, Nakashima Y. The incidence and risk factors for venous obstruction after implantation of transvenous pacing leads. Pacing Clin Electrophysiol. 2002;25:1605–11.

Rozmus G, Daubert JP, Huang DT, Rosero S, Hall B, Francis C. Venous thrombosis and stenosis after implantation of pacemakers and defibrillators. J Interv Card Electrophysiol. 2005;13:9–19.

Smith HJ, Fearnot NE, Byrd CL, Wilkoff BL, Love CJ, Sellers TD. Five-years experience with intravascular lead extraction. US lead extraction database. Pacing Clin Electrophysiol. 1994;17:2016–20.

Sticherling C, Chough SP, Baker RL, Wasmer K, Oral H, Tada H, Horwood L, Kim MH, Pelosi F, Michaud GF, Strickberger SA, Morady F, Knight BP. Prevalence of central venous occlusion in patients with chronic defibrillator leads. Am Heart J. 2001;141:813–6.

Taylor CA, Hughes TCR, Zarins CK. Finite element modeling of blood flow in arteries. Comput Methods Appl Mech Eng. 1998a;158:155–96.

Taylor CA, Hughes TJ, Zarins CK. Finite element modeling of three-dimensional pulsatile flow in the abdominal aorta: relevance to atherosclerosis. Ann Biomed Eng. 1998b;26:975–87.

Taylor CA, Draney MT, Ku JP, Parker D, Steele BN, Wang K, Zarins CK. Predictive medicine: computational techniques in therapeutic decision-making. Comput Aided Surg. 1999;4:231–47.

van Rooden CJ, Molhoek SG, Rosendaal FR, Schalij MJ, Meinders AE, Huisman MV. Incidence and risk factors of early venous thrombosis associated with permanent pacemaker leads. J Cardiovasc Electrophysiol. 2004;15:1258–62.

Wilkoff BL, Byrd CL, Love CJ, Hayes DL, Sellers TD, Schaerf R, Parsonnet V, Epstein LM, Sorrentino RA, Reiser C. Pacemaker lead extraction with the laser sheath: results of the pacing lead extraction with the excimer sheath (PLEXES) trial. J Am Coll Cardiol. 1999;33:1671–6.

Wilkoff BL, Belott PH, Love CJ, Scheiner A, Westlund R, Rippy M, Krishnan M, Norlander BE, Steinhaus B, Emmanuel J, Zeller PJ. Improved extraction of ePTFE and medical adhesive modified defibrillation leads from the coronary sinus and great cardiac vein. Pacing Clin Electrophysiol. 2005;28:205–11.

Wilson N, Wang K, Dutton R, Taylor CA. A software framework for creating patient specific geometric models from medical imaging data for simulation based medical planning of vascular surgery. Lect Notes Comput Sci. 2001;2208:449–56.

Wilson NM, Arko FR, Taylor CA. Predicting changes in blood flow in patient-specific operative plans for treating aortoiliac occlusive disease. Comput Aided Surg. 2005;10:257–77.